

18-4-2005

A new methodology for deformable object simulation

Yongmin Zhong
Monash University

Bijan Shirinzadeh
Monash University

Gursel Alici
University of Wollongong, gursel@uow.edu.au

Julian Smith
Monash University

Follow this and additional works at: <https://ro.uow.edu.au/engpapers>



Part of the [Engineering Commons](#)

<https://ro.uow.edu.au/engpapers/80>

Recommended Citation

Zhong, Yongmin; Shirinzadeh, Bijan; Alici, Gursel; and Smith, Julian: A new methodology for deformable object simulation 2005.
<https://ro.uow.edu.au/engpapers/80>

A New Methodology for Deformable Object Simulation*

Yongmin Zhong¹, Bijan Shirinzadeh¹, Gursel Alici², Julian Smith³

¹Robotics & Mechatronics Research
Laboratory

Monash University
VIC 3800, Australia

Bijan.Shirinzadeh@eng.monash.edu.au

²School of Mechanical, Materials,
and Mechatronics Engineering

University of Wollongong
2522 NSW, Australia

gursel@uow.edu.au

³Department of Surgery
Monash Medical Centre

Monash University
VIC 3800, Australia

Julian.Smith@med.monash.edu.au

Abstract – This paper presents a new methodology for the deformation of soft objects by drawing an analogy between heat conduction and elastic deformation. The potential energy stored in an elastic body as a result of a deformation caused by an external force is propagated among mass points by the principle of heat conduction. An improved heat conduction model is developed for propagating the energy generated by the external force in a natural manner. A method is presented to derive the internal forces from the potential energy distribution. This methodology not only deals with large-range deformation, but also accommodates both isotropic and anisotropic materials by simply changing thermal conductivity constants. Examples are presented to demonstrate the efficiency of the proposed methodology.

Index Terms – deformation, soft objects, surgery simulation and analogous systems.

I. INTRODUCTION

Virtual reality based surgery simulation is expected to provide benefits in many aspects of surgical procedure training and evaluation. Research efforts have been dedicated to simulating the behaviours of deformable objects. These methods can be divided into two types. One is focused on real-time simulation, such as mass-spring models [1, 2] and spline surfaces used in deformation [3, 4]. The advantage of this model is that the computation is less time consuming and the algorithm is easier to be implemented. However, these methods do not allow accurate modelling of material properties and increasing the number of springs leads to a stiffer system. Another is devoted to accurate deformation modelling, such as Finite Element Method (FEM) [5, 6] and Boundary Element Method (BEM) [7, 8]. In FEM or BEM, rigorous mathematical analysis based on continuum mechanics is applied to accurately model the mechanical behaviours of soft objects. However, these methods are computationally expensive and are typically simulated off-line. The pre-calculation [7], matrix condensation [9] and the space and time adaptive level of detail technique [10] are used to enhance the computational performance.

In general, most of the existing methods for soft object deformation are fully built on an elastic model that is an ideal tool to describe the deformation. However, the behaviours of soft objects such as human tissues are extremely nonlinear [11, 12]. The common deformation methods, such as mass-spring, FEM and BEM, are mainly built on linear elastic models because of the simplicity of linear elastic models and also because linear elastic models permit to reduce runtime computation. However, linear elastic models cannot accommodate the large-range

geometric deformation. Although the few methods built on the nonlinear elastic model can handle the large-range deformation [13], the use of quadric strains generally causes a very expensive computation for real-time simulation. In addition, extra work often needs to be performed for anisotropic deformation.

This paper presents a new methodology for deformable object simulation by drawing an analogy between heat conduction and elastic deformation. The deformation is formulated as heat conduction. The potential energy stored due to a deformation caused by an external force is calculated and treated as the heat energy injected into the system with respect to the first law of thermodynamics. The principle of heat conduction is used to propagate the potential energy generated by the external force among mass points. An improved heat conduction model is developed for propagating the energy in a natural manner. A method is presented to derive the internal forces from the potential energy distribution. This methodology can not only deal with large-range deformation due to the natural energy distribution of heat conduction, but also can accommodate both isotropic and anisotropic materials easily through simply changing the conductivity constants.

There are several investigations that combine heat conduction with deformable modelling. However, these are mainly focused on fluid modelling [14, 15, 16] and temperature produced by heat conduction is used to model the viscoelasticity of fluid or change the stiffness of springs. To the best of our knowledge, this study is the first to directly use heat conduction techniques to mimic the deformation of soft objects under externally applied loads.

II. DESIGN OF HEAT CONDUCTION MODEL

A. The heat conduction analogy

We formulate the deformation of soft objects as a heat conduction problem. The heat conduction provides a natural way for energy propagation according to the inherent property of materials, i.e. the thermal conductivity. The thermal conductivity determines the temperature distribution in the field. Heat flux is a vector in the sense that it points in the direction of a negative temperature gradient. It is generated by a source, always flows from high temperature points to low temperature points and finally flows into a sink. The flow of heat flux is an optimum consequence generated by a thermal energy distribution.

In addition, the internal energy of heat conduction is changed with time. The heat conduction dynamics provides a description of deformation process and also has fast

* This work is supported by Australian Research Council

response to variations in the environments. This feature is very suitable for real-time deformation accommodating the variable external force.

In the proposed heat conduction analogy, the deformation of soft objects is treated as heat conduction with a heat source/sink at the contact point. The energy generated by the external force is treated as a heat source/sink at the contact point depending on the external force being a stressed/tensile force, and the object surface is treated as a heat field. As a result of a heat conduction process, a heat field is developed on the object surface. The heat flux that originates from the heat source or ends at the heat sink always flows from the point with a high potential energy to the point with a low potential energy. If the flow of heat flux is further thought to be caused by the internal forces, such a field with heat source/sink, heat flux and the flow of heat flux can be seen as a communication medium among an external force, internal forces and deformation.

B. Heat Conduction Model Design

The heat conduction is performed on the object surface as a 2D heat conduction. The 2D heat conduction having a continually internal heat sources is described by a partial differential equation of the second order

$$\left(k_u \frac{\partial^2 T}{\partial u^2} + k_v \frac{\partial^2 T}{\partial v^2} \right) + q = \alpha \frac{\partial T}{\partial t} \quad (1)$$

$$\vec{r} = -k \nabla T$$

where T is the temperature of the observed point with coordinates u and v at time t , k_u and k_v are the thermal conductivity of the observed point in the u and v directions at time t , and q is the heat flow rate (heat divided by area) of internal heat sources ($q > 0$) or sinks ($q < 0$) at time t . α is a constant called the thermal capacity. \vec{r} is the heat flux at time t , which is the negative gradient of temperature. ∇ represents the gradient operator.

For isotropic deformable objects, there is $k_u = k_v = k$. Therefore, Eq. (1) becomes:

$$k \left(\frac{\partial^2 T}{\partial u^2} + \frac{\partial^2 T}{\partial v^2} \right) + q = \alpha \frac{\partial T}{\partial t} \quad (2)$$

For the sake of convenient description, the deformable object refers to an isotropic deformable object unless we declare it as anisotropic.

To solve Eq. (1), it is necessary to determine the boundary conditions. The boundary conditions determine the character of the heat interchange over the boundary. In the case of soft object deformation, the boundary can be treated as the part of the soft object that connects/contacts with other objects. For simplicity, we choose the Dirichlet boundary conditions, i.e. the specified temperature on the boundary Ω :

$$T = T_\Omega \quad \text{on } \Omega \quad (3)$$

where T_Ω is the given boundary temperature function.

III. CONSTRUCTION OF HEAT CONDUCTION MODEL

A. Setting Heat Rate

When a soft object is deformed under an external force, there is a displacement observed. Therefore, the deformation can be regarded as to be generated by the work done by the external force. According to the first law of thermodynamics, the work done by the external force can be transformed into an equivalent heat at the contact point. Therefore, the heat rate q is

$$q = \frac{\vec{F} \bullet \vec{S}}{A_F} \quad (4)$$

where \vec{F} is the external force, \vec{S} is the displacement and A_F is the area on which the external force is applied.

If the external force is applied to a point or the area that the force is applied on is small, the heat rate q may be regarded as the elastic potential energy at the contact point:

$$q = \sigma \varepsilon = \sum_{i=1}^3 \sum_{j=1}^3 \sigma_{ij} \varepsilon_{ij} \quad (5)$$

where σ is the stress tensor and ε is the strain tensor at the contact point. The commonly used and simple strain tensor is linear Cauchy strain tensor described by:

$$\varepsilon = \frac{1}{2} \left(\frac{\partial u_i}{\partial x_j} + \frac{\partial u_j}{\partial x_i} \right) \quad (6)$$

A straight forward approach that leads to a linear relationship between these two tensors is provided by the Hooke's law:

$$\sigma = C \varepsilon \quad (7)$$

For isotropic materials, Eq. (7) can be further written in components as:

$$\sigma_{ij} = \delta_{ij} \lambda \sum_k \varepsilon_{kk} + 2\mu \varepsilon_{ij} \quad (8)$$

where δ is the Kronecker delta, λ and μ are the two l ame constants.

From Eq. (7) and (8), we can deduce the displacement from the given external force and the heat rate q can be subsequently obtained.

In ordinary heat conduction, the heat rate is the same value at each mass point. For our purpose, the energy generated by the external force is treated as a heat source and propagated to other mass points along the object surface. Therefore, the obtained heat rate is set only at the contact point of the external force, and the values of the heat rate at other mass points are set to zero.

B. Heat Conduction Model Design

In 2D heat conduction, the heat conduction model is usually constructed on a 2D rectangular net. However, here the heat conduction model is constructed on the 3D object surface model.

1) *Heat Conduction Model on Rectangular Nets*: If the object surface model is a rectangular net, the heat conduction equation for each internal node can be established using a finite-difference scheme. For point $\vec{P}_{i,j}$ shown in Fig. 1, the heat conduction equation is shown in Eq. (9).

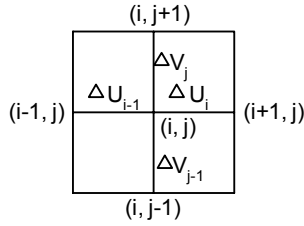


Fig. 1 Heat conduction model on a rectangular net

$$\begin{aligned}
 & \frac{kT_{i+1,j}(n\Delta t)}{\Delta U_i(\Delta U_{i-1} + \Delta U_i)} + \frac{kT_{i-1,j}(n\Delta t)}{\Delta U_{i-1}(\Delta U_{i-1} + \Delta U_i)} \\
 & + \frac{kT_{i,j+1}(n\Delta t)}{\Delta V_j(\Delta V_{j-1} + \Delta V_j)} + \frac{kT_{i,j-1}(n\Delta t)}{\Delta V_{j-1}(\Delta V_{j-1} + \Delta V_j)} \\
 & - \frac{kT_{i,j}(n\Delta t)}{\Delta U_{i-1}\Delta U_i} - \frac{kT_{i,j}(n\Delta t)}{\Delta V_{j-1}\Delta V_j} + \frac{q}{2} \\
 & = \frac{\alpha}{2\Delta t} [T_{i,j}((n+1)\Delta t) - T_{i,j}(n\Delta t)] \\
 & \Delta U_{i-1} = \left\| \overrightarrow{P_{i-1,j}P_{i,j}} \right\| \quad \Delta U_i = \left\| \overrightarrow{P_{i,j}P_{i+1,j}} \right\| \\
 & \Delta V_{j-1} = \left\| \overrightarrow{P_{i,j-1}P_{i,j}} \right\| \quad \Delta V_j = \left\| \overrightarrow{P_{i,j}P_{i,j+1}} \right\|
 \end{aligned} \tag{9}$$

where Δt is a constant time step, $T_{i,j}(n\Delta t)$ is the temperature at point $\vec{P}_{i,j}$ at the time $n\Delta t$, $\left\| \overrightarrow{P_{i-1,j}P_{i,j}} \right\|$ and other similar terms represent the magnitudes of the vector $\overrightarrow{P_{i-1,j}P_{i,j}}$ and other similar vectors.

For anisotropic materials, since the conductivity at each node is different, the heat conduction equation for each internal node may be described by the following:

$$\begin{aligned}
 & \frac{k_{i+1,j}T_{i+1,j}(n\Delta t)}{\Delta U_i(\Delta U_{i-1} + \Delta U_i)} + \frac{k_{i-1,j}T_{i-1,j}(n\Delta t)}{\Delta U_{i-1}(\Delta U_{i-1} + \Delta U_i)} \\
 & + \frac{k_{i,j+1}T_{i,j+1}(n\Delta t)}{\Delta V_j(\Delta V_{j-1} + \Delta V_j)} + \frac{k_{i,j-1}T_{i,j-1}(n\Delta t)}{\Delta V_{j-1}(\Delta V_{j-1} + \Delta V_j)} \\
 & - \frac{k_{i,j}T_{i,j}(n\Delta t)}{\Delta U_{i-1}\Delta U_i} - \frac{k_{i,j}T_{i,j}(n\Delta t)}{\Delta V_{j-1}\Delta V_j} + \frac{q}{2} \\
 & = \frac{\alpha}{2\Delta t} [T_{i,j}((n+1)\Delta t) - T_{i,j}(n\Delta t)]
 \end{aligned} \tag{10}$$

where $k_{i,j}$ is the conductivity at point $\vec{P}_{i,j}$.

2) *Heat Conduction Model on Triangular Nets*: If the object surface is a locally or globally triangular net, a concept of control area [17] is used to aid establishing the

heat conduction equation at each node. The heat conduction equation for each node can be derived by energy balance at the node. For example, as shown in Fig. 2, the control area of point \vec{P}_0 is constructed by connecting each intersection points between the perpendicular centerlines of each edges adjacent to point \vec{P}_0 , i.e. S_{abcdef} . The heat conduction equation at point \vec{P}_0 is

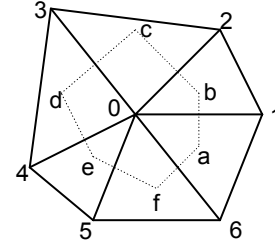


Fig. 2 Heat conduction model on a triangular net

$$\begin{aligned}
 & \frac{L_{ab}}{L_{01}} [(T_1(n\Delta t) - T_0(n\Delta t))k] + \frac{L_{bc}}{L_{02}} [(T_2(n\Delta t) - T_0(n\Delta t))k] \\
 & + \frac{L_{cd}}{L_{03}} [T_3(n\Delta t) - T_0(n\Delta t)]k + \frac{L_{de}}{L_{04}} [T_4(n\Delta t) - T_0(n\Delta t)]k \\
 & + \frac{L_{ef}}{L_{05}} (T_5(n\Delta t) - T_0(n\Delta t))k + \frac{L_{fa}}{L_{06}} (T_6(n\Delta t) - T_0(n\Delta t))k \\
 & + qS_{abcdef} = \frac{\alpha}{\Delta t} [T_0((n+1)\Delta t) - T_0(n\Delta t)]
 \end{aligned} \tag{11}$$

where $L_{nm} = \left\| \overrightarrow{P_m P_n} \right\|$ is the distance between two points \vec{P}_m and \vec{P}_n .

In the similar way as Eq. (10), the heat equation at point \vec{P}_0 for anisotropic materials can be given as

$$\begin{aligned}
 & \frac{L_{ab}}{L_{01}} [k_1 T_1(n\Delta t) - k_0 T_0(n\Delta t)] + \frac{L_{bc}}{L_{02}} [k_2 T_2(n\Delta t) - k_0 T_0(n\Delta t)] \\
 & + \frac{L_{cd}}{L_{03}} [k_3 T_3(n\Delta t) - k_0 T_0(n\Delta t)] + \frac{L_{de}}{L_{04}} [k_4 T_4(n\Delta t) - k_0 T_0(n\Delta t)] \\
 & + \frac{L_{ef}}{L_{05}} [k_5 T_5(n\Delta t) - k_0 T_0(n\Delta t)] + \frac{L_{fa}}{L_{06}} (k_6 T_6(n\Delta t) - k_0 T_0(n\Delta t)) \\
 & + qS_{abcdef} = \frac{\alpha}{\Delta t} [T_0((n+1)\Delta t) - T_0(n\Delta t)]
 \end{aligned} \tag{12}$$

where k_i is the conductivity at point \vec{P}_i .

IV. INTERNAL FORCE DERIVATION AND MODEL DYNAMICS

A. Internal Force Derivation

Potential functions provide an elegant method of describing internal forces based on point positions. For a potential function ϕ , the force exerted on a point \vec{P}_i is due to the gradient of the potential energy ϕ with respect to the change in position.

$$\vec{f} = -\nabla_{\vec{P}_i} \phi$$

$$\nabla_{\vec{P}_i} \phi = \left(\frac{\partial \phi}{\partial \vec{P}_{ix}}, \frac{\partial \phi}{\partial \vec{P}_{iy}}, \frac{\partial \phi}{\partial \vec{P}_{iz}} \right) \quad (13)$$

The heat potential field generated by heat conduction describes the energy distribution on the object surface. The associated potential function is temperature. According to the first law of thermodynamics, the heat potential at each point can be transformed into an equivalent elastic potential. Therefore, the internal elastic force at a point can be represented by the negative gradient of the temperature, i.e. the heat flux at this point.

$$f = -k \nabla_{\vec{P}_i} T \quad (14)$$

For anisotropic materials, Eq. (13) becomes

$$f = -\nabla_{\vec{P}_i} kT \quad (15)$$

Since heat flux flows along an edge from a high temperature point to a low temperature point, the internal force at a point is derived from the neighboring points of this point. The force between any adjacent points is calculated as follows:

For any two adjacent points \vec{P}_i and \vec{P}_j , and assuming that the temperatures at these two points are $T_{\vec{P}_i}$ and $T_{\vec{P}_j}$, the temperature at any point \vec{P} between these two points is regarded as a function of the distance between point \vec{P}_i and point \vec{P} . Therefore, the following relationships may be written:

$$T = T(l)$$

$$l = \left\| \vec{P} - \vec{P}_i \right\| \quad (16)$$

Thus:

$$\nabla_{\vec{P}_i} T = \frac{dT}{dl} \nabla_{\vec{P}_i} l = - \frac{\left| T_{\vec{P}_j} - T_{\vec{P}_i} \right|}{\left\| \vec{P}_j - \vec{P}_i \right\|} \vec{P}_i \vec{P}_j \quad (17)$$

where $\vec{P}_i \vec{P}_j = \frac{\vec{P}_j - \vec{P}_i}{\left\| \vec{P}_j - \vec{P}_i \right\|}$ and $\left| T_{\vec{P}_j} - T_{\vec{P}_i} \right|$ is the magnitude of the temperature change between point \vec{P}_i and point \vec{P}_j .

Therefore, the force between point \vec{P}_i and point \vec{P}_j is

$$\vec{f}_{ij} = k \frac{\left| T_{\vec{P}_j} - T_{\vec{P}_i} \right|}{\left\| \vec{P}_j - \vec{P}_i \right\|} \vec{P}_i \vec{P}_j \quad (18)$$

The internal force \vec{g}_i at a given point \vec{P}_i is the sum of the internal forces from all adjacent points of point \vec{P}_i .

$$\vec{g}_i = \sum_{j \in N(\vec{P}_i)} \vec{f}_{ij} \quad (19)$$

where $N(\vec{P}_i)$ is the neighbor points of \vec{P}_i , \vec{f}_{ij} is the force between point \vec{P}_i and its neighbor point \vec{P}_j .

B. Model Dynamics

When an external force is applied to a soft object, the contact point of the external force is replaced with a new position. As a result, the other points not influenced by the external force are in an unstable state. The energy generated by the external force is propagated through heat conduction among mass points to establish a new equilibrium state by generating the corresponding internal forces. Effectively, the new position of each point is obtained based on the equilibrium state. The physically dynamic process is governed by the Lagrangian equation of motion of each node:

$$m_i \frac{d^2 \vec{P}_i}{dt^2} + \gamma_i \frac{d \vec{P}_i}{dt} + \vec{g}_i = \vec{F}_i \quad (20)$$

where \vec{P}_i is the position vector of node i, m_i and γ_i are the mass and damping constant of the node i, respectively. \vec{g}_i is the net internal force applied to node i at time t, and \vec{F}_i is the external force applied to node i at time t.

The solution of Eq. (20) can be computed either by implicit integration scheme or explicit integration scheme. Although the implicit integration has the advantage of being unconditionally stable, which means it allows large time steps to be used, it is computationally intensive and requires inverting a sparse matrix at each iteration [18]. Therefore, the explicit integration scheme is adopted to solve the Eq. (20). The advantage of the explicit scheme is that no rigid matrix inversion is required for updating each vertex.

The second-order differential equations can be divided into a system of first order differential equations by introducing a velocity function \vec{V}_i .

$$\frac{d \vec{P}_i}{dt} = \vec{V}_i$$

$$\frac{d \vec{V}_i}{dt} = \frac{\vec{F}_i - \vec{g}_i - \gamma_i \vec{V}_i}{m_i} \quad (21)$$

The explicit Euler integration scheme is used to numerically solve Eq. (21).

$$\vec{V}_i^{n+1} = \vec{V}_i^n + \Delta t \frac{\vec{F}_i - \vec{g}_i - \gamma_i \vec{V}_i}{m_i} \quad (22)$$

$$\vec{P}_i^{n+1} = \vec{P}_i^n + \Delta t \vec{V}_i^n$$

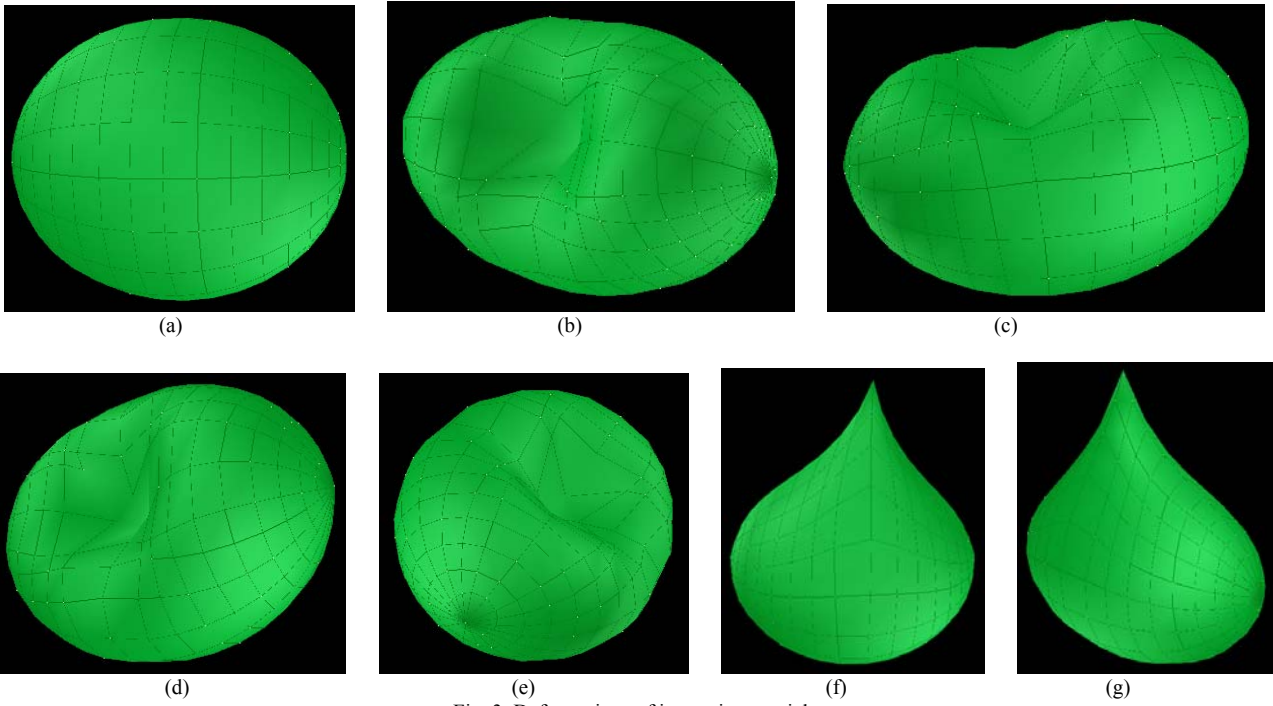


Fig. 3 Deformations of isotropic materials

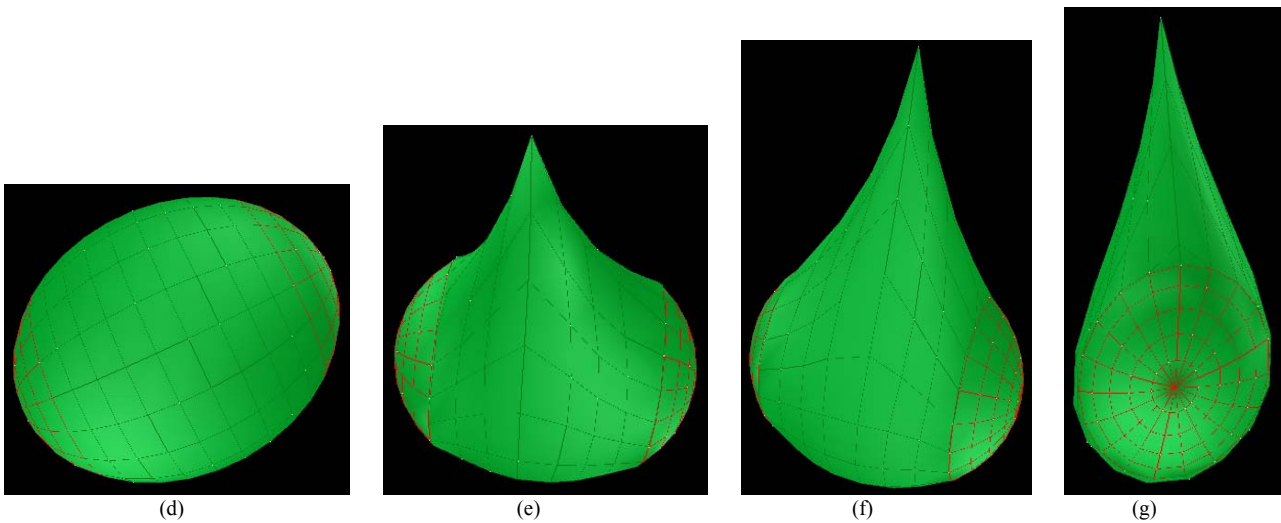
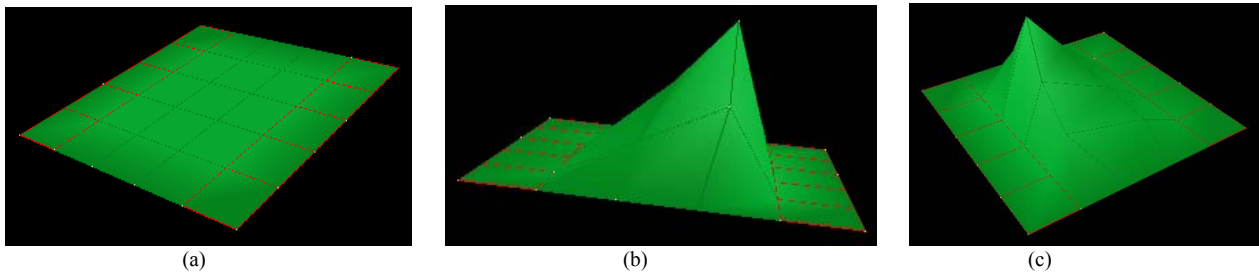


Fig. 4 Deformations of anisotropic materials

V. IMPLEMENTATION AND DISCUSSIONS

A prototype system has been implemented for interactive deformable simulation. Experiments are conducted to investigate isotropic deformation, anisotropic deformation and the non-linear load-deformation of the model.

Fig. 3 illustrates the deformations of an isotropic material modelled with 400 mass points (the thermal

conductivity = 0.4 and the damping = 10). Fig. 3(a) shows the undeformed object whose shape is a superquadric. Fig. 3(b), (c), (d) and (e) are different views of the object deformed under a compressive force. Fig. 3(f) and (g) are the objects deformed under a tensile force.

The behaviour of anisotropic materials can be easily simulated by the proposed model through simply setting different conductivities. Fig. 4 illustrates the deformations of anisotropic materials. The red parts of the images have a

very low conductivity and are not deformed by the external forces. Fig. 4(a) shows a plane with different conductivities. Fig. 4(b) and (c) are the deformation of the plane under a tensile force. Fig. 4(d) shows the same object in Fig. 3(a) but with different conductivities. Fig. 4(e), (f) and (g) show the different views of the object deformed under a tensile force.

The proposed model has been tested to determine if it exhibits non-linear load-deformation relationship. Eight materials that are modelled with different damping constants (from right to left in Fig. 5, the damping is 1.0, 2.0, 4.0, 5.0, 6.0, 7.0, 9.0 and 10.0, respectively) are tested. The deformation is calculated when the force applied to the model is increased at a constant rate. The results in Fig. 5 demonstrate that deformation varies non-linearly with the applied force.

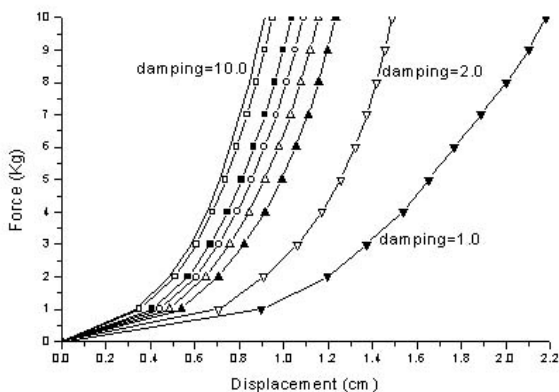


Fig. 5 Non-linear load-deformation relationship

With the deformable modelling examples, it is observed that most of the deformation simulation time is spent on solving the heat conduction equation by the refined Gaussian elimination whose calculation speed is $O(N^2)$. The efficiency of solving the heat equation could be further improved to $O(N)$ by a neural network algorithm [19].

Compared with most of the existing deformation methods such as mass-spring, BEM and linear FEM, the methodology can perform large-range displacements through its non-linear load-deformation relationship. Compared with non-linear FEM such as [13], the heat conduction model provides for greater ease in formulation than the complex non-linear elastic model, and only surface mass points are involved in computation and rendering without any inside points while the interior has to be meshed and calculated in FEM. In addition, the methodology can easily accommodate anisotropic materials by simply setting conductivities while extra work has to be performed in both mass-spring and FEM.

VI. CONCLUSIONS

Presented in this paper is a new methodology to mimic the deformation of soft objects by drawing an analogy between heat conduction and elastic deformation. The contribution of this paper is that heat conduction techniques are used to naturally propagate the energy generated by the external force to extrapolate internal forces. An improved heat conduction model is developed for the natural propagation of the energy generated by the external force. A method is presented for deriving the internal forces from the

potential energy distribution. This methodology can not only deal with large-range deformation due to the natural thermal distribution of heat conduction, but also can accommodate both isotropic and anisotropic materials through simply changing the conductivity constants.

Ongoing research includes the improvement of the computational efficiency with a neural network algorithm and the integration of the virtual surgery environment with the Phantom haptic device for force feedback.

ACKNOWLEDGMENT

This research is supported by Australian Research Council (ARC).

REFERENCES

- [1] C. Paloc, F. Bello, R. I. Kitney and A. Darzi, "Online multiresolution volumetric mass spring model for real time soft tissue deformation", Lecture Notes in Computer Science, vol. 2489, 2002, pp. 219-226
- [2] K. Choi, H. Sun and P. A. Heng, "Interactive deformation of soft tissues with haptic feedback for medical learning", IEEE Transaction on Information Technology in Biomedicine, vol. 7, no. 4, 2003, pp.358-363
- [3] U. Bockholt, W. Müller and G. Voss (etc.), Real-time simulation of tissue deformation for the nasal endoscopy simulator (NES), Computer aided surgery, vol. 4, no. 5, 1999, pp. 281-285
- [4] J. S. Rotnes, J. Kaasa and G. Westgaard (etc.), "Realism in surgical simulators with free-form geometric modeling", International Congress Series, vol. 1230, 2001, pp. 1032-1037
- [5] S. Cotin, H. Delingette and N. Ayache, "A hybrid elastic model allowing real-time cutting, deformations and force-feedback for surgery training and simulation", The Visual Computer, vol. 16, no. 8, 2000, pp.437-452
- [6] C. Basdogan, S. De and J. Kim (etc.), "Haptics in minimally invasive surgical simulation and training", IEEE Computer Graphics and Applications, vol. 24, no. 2, 2004, pp. 56-64
- [7] D. James and D. Pai, "Artdefo accurate real time deformable objects", Proceedings of the 26th annual conference on Computer graphics and interactive techniques, Los Angeles, USA, 1999, pp. 65-72
- [8] C. Monserrat, U. Meier and M. Alcaniz (etc.), "A new approach for the real-time simulation of tissue deformations in surgery simulation", Computer Methods and Programs in Biomedicine, vol. 64, 2001, pp. 77-85
- [9] M. Bro-Nielsen, "Finite element modeling in surgery simulation", Proceedings of The IEEE, vol. 86, no. 3, 1998, pp. 490-503
- [10] G. Debunne, M. Desbrun, M. P. Cani and A. H. Barr, "Dynamic real-time deformations using space & time adaptive sampling", ACM SIGGRAPH 2001, Los Angeles, USA, pp. 31-36
- [11] Y. C. Fung, "Biomechanics: Mechanical properties of living tissues", Second Edition, New York: Springer-Verlag, 1993
- [12] R. M. Kenedi, T. Gibson, J. H. Evans and J. C. Barbenel, "Tissues mechanics", Physics in Medicine & Biology, vol. 20, no. 5, 1975, pp. 699-717
- [13] G. Picinbono, H. Delingette and N. Ayache, "Non-linear anisotropic elasticity for real-time surgery simulation", Graphical Models, vol. 65, no. 5, 2003, pp. 305-321
- [14] D. Terzopoulos, J. Platt and K. Fleischer, "Heating and melting deformable models," The Journal of Visualization and Computer Animation, vol. 2, no. 2, 1991, pp. 68-73
- [15] D. Stora, P.-O. Agliati, M.-P. Cani and F. Neyret, "Animating Lava Flows", Proc. of Graphics Interface, Kingston, Ontario, Canada, June 1999, pp. 203-210.
- [16] M. Carlson, P. J. Mucha, R. B. Van Horn and G. Turk, "Melting and flowing", Proceedings of the 2002 ACM SIGGRAPH/Eurographics symposium on Computer animation, 2002, pp. 167-202
- [17] D. R. Croft and D. G. Lilley, "Heat transfer calculations using finite difference equations", Applied Science Publishers Ltd, London, 1977
- [18] D. Baraff and A. Witkin, "Large steps in cloth simulation", Proceedings of SIGGRAPH'98, pp. 43-54
- [19] L. O. Chua and L. Yang, "Cellular neural network: Theory", IEEE Transactions on Circuits and Systems, Vol. 35, No. 10, 1988, pp1257-1272